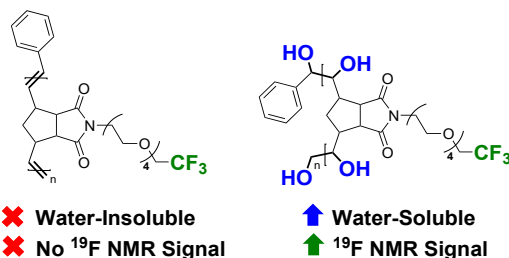


Polymeric ^{19}F MRI Contrast Agents Prepared with Ring-Opening Metathesis Polymerization/Dihydroxylation

Iris K. Tennie and Andreas F. M. Kilbinger*

Department of Chemistry, University of Fribourg, Chemin du Musée 9, CH-1700 Fribourg, Switzerland

E-mail: andreas.kilbinger@unifr.ch



Abstract

The capability of ring-opening metathesis polymerization (ROMP) to efficiently incorporate bulky monomers and conserve olefin bonds during polymerization was exploited to design water-soluble fluoropolymers, which were evaluated as potential quantitative ^{19}F magnetic resonance imaging (MRI) contrast agents. The fluoromonomeric units were comprised of either 3, 6, 9 or 18 magnetically equivalent fluorine atoms. Aqueous solubility was achieved through dihydroxylation of the partially unsaturated polymeric backbone and by either TEG-based linker incorporation, ammonium quaternization or copolymerization.

Introduction

Magnetic resonance imaging (MRI) plays an important role in detection of various diseases. Metal-based contrast agents, such as gadolinium(III) complexes, are often used to lower the detection limit in ^1H MRI and enhance the image contrast.¹ Especially in the unchelated form, they have, however, been associated with safety concerns, including prolonged accumulation within the body and nephrogenic systemic fibrosis.² With excellent sensitivity second only to ^1H nucleus, negligible background signal and a wide chemical shift range, it is possible to track ^{19}F MRI contrast agents in a quantitative manner.³

While the ^1H MRI image is mostly composed of the NMR signal of water protons, the ^{19}F MRI image directly depicts the fluorinated contrast agent. The image intensity is thus dependent on the concentration of the NMR detectable ^{19}F nuclear spins as well as on the longitudinal T_1 and transverse T_2 relaxation times of the fluorinated moiety. These are extremely sensitive to the internal mobility and spatial arrangement of the nuclear spins as well as to the dipole-dipole and the Zeeman interaction with the applied magnetic field. To achieve optimal signal intensity, T_1/T_2 ratio should be near one. This requires decreasing T_1 and increasing T_2 as much as possible when designing fluorinated contrast agents. Aggregation of the nuclei, on the other hand, leads to a reduced T_2 , severe line broadening and diminution of the NMR signal.^{4,5}

One of the strategies to prevent aggregation is to deliver highly fluorinated probes such as perfluorooctyl bromide,⁶ perfluoropolyether (PFPE),⁷ perfluoro-15-crown-5-ether⁸ and PERFECTA (36 equivalent ^{19}F atoms)⁹ as nanoemulsions with a droplet size in the range of 100-200 nm. Such emulsions are very lipophilic with long retention times in internal organs and unstable especially in blood.¹⁰

Emulsion formulation can be avoided by enhancing aqueous solubility by designing amphiphilic tetraethylene glycol (TEG)-based fluorinated molecular probes,¹¹ liposomal formulations with hydrophilic fluorinated molecules¹² or incorporating poly(ethylene glycol) (PEG) units on the periphery of dendritic probes.¹³ Alternatively, sulfoxide-containing² statistical

copolymers, block copolymers of poly(acrylic acid)¹⁴ or PEG-114¹⁵ as well as PEG-8¹⁶ and PEG-400¹⁷ units in hyperbranched polymers were implemented to prevent aggregation of fluorinated units. All these polymers were prepared by either reversible addition-fragmentation chain transfer (RAFT) or atom transfer radical (ATRP) polymerization, whereby mainly commercially available 2,2,2-trifluoroethyl (meth)acrylate monomers^{2,14,16,17} were used as fluorinated reporters. Despite the incorporation of water-solubilizing segments most of these copolymers exhibit low ¹⁹F T_2 values and high T_1/T_2 ratios in aqueous solutions. It is only very recently that water-soluble 2,2,2-trifluoroethyl acrylamide-based homofluoropolymers featuring polar sulfoxide groups have been prepared by Whittaker and colleagues.¹⁸

Ring opening metathesis polymerization (ROMP), on the other hand, is known as one of the fastest, most versatile and functional-group-tolerant polymerization approaches that is also capable of efficiently polymerizing bulky monomers. Polydispersities are low and the polymerization degrees can be precisely controlled by altering the monomer to catalyst ratio, whereby monomers can be comprised of mono- or oligo-cyclic olefins.¹⁹ Among these, a range of norbornene-imides have been successfully applied to prepare fluorine-18 nanoprobe for positron emission tomography²⁰ as well as Gd³⁺-DOTA-based²¹ and nitroxide-based²² ¹H MRI contrast agents. Another very useful property of ROMP is the conservation of main chain olefin bonds during the polymerization. Dihydroxylation of such double bonds catalyzed by osmium tetroxide has been shown to improve aqueous solubility.²³⁻²⁵ Although this feature offers great possibilities to completely alter the polarity of the polymeric backbone, it has mostly been overlooked and not fully explored.

In this work, water-soluble ¹⁹F MRI contrast agents have been prepared by dihydroxylation of the main chain olefins in fluorinated ROMP polymers. This was achieved without the need of additional solubilizing segments. Polymers with higher fluorine content (>21 wt %), on the other hand, did require additional modifications such as quaternization of the tertiary amines or copolymerization with hydrophilic TEG-based monomers. In copolymers, a linear dependence of ¹⁹F NMR signal intensity on polymer content was observed in a wide

range of molecular masses.

Experimental Section

Materials. 2,2,2-trifluoroethanol (Fluorochem, 99 %), ethylene carbonate (Alfa Aesar, 99 %), diisopropyl azodicarboxylate (DIAD; Fluorochem, 99 %), di-*tert*-butylazodicarboxylate (DBAD; Fluorochem, 98 %), triethylamine (Fluorochem, 99 %), *N*-(3-aminopropyl)diethanolamine (Fluorochem, 95 %), perfluoro-*tert*-butanol (Fluorochem, 97 %), methanesulfonyl chloride (Sigma-Aldrich, 99 %), ethyl vinyl ether (Sigma-Aldrich, 99 %), ethanolamine, potassium osmate(VI) dihydrate (Sigma-Aldrich), 4-methylmorpholine *N*-oxide (Sigma-Aldrich, 97 %), Grubbs' second generation catalyst (**G2**; Sigma-Aldrich), *cis*-norbornene-*exo*-2,3-dicarboxylic anhydride (Carbosynth), 1-amino-3,6,9-trioxaundecanyl-11-ol (amino-TEG-alcohol; Combi-Blocks, 95 %), MeO-PEG4-NH₂ (Combi-Blocks, 97 %) and deuterated solvents (CDCl₃, CD₂Cl₂, D₂O, CD₃COCD₃, CD₃OD and DMSO-*d*₆; Cambridge Isotope Laboratories) were used as received without further purification. Grubbs' third generation catalyst (**G3**) was synthesized from **G2** by reaction with 5-bromopyridine (Fluorochem, 97 %) at RT and purified by filtration with dry pentane. *N*-(Hydroxyethyl)-*cis*-norbornene-*exo*-2,3-dicarboxiimide (**S2**)²⁶ and *exo-N*-methyl-norbornene-2,3-dicarboxiimide (**M0**)²⁷ were prepared as reported previously. Flash chromatography was performed on silica gel (SiliCycle, 230-400 mesh, particle size 32-63 μm, 60 Å). Residual ruthenium and osmium amounts were removed from the polymers by SiliaMetS DMT (SiliCycle), which is a silica-bound 2,4,6-trimercaptotriazine. SnakeSkin dialysis tubing, 3.5K MWCO, 22 mm, was purchased from Thermo Fisher Scientific.

2-(2,2,2-trifluoroethoxy)ethyl-*cis*-norbornene-*exo*-2,3-dicarboxiimide (M1).

S1.1 was obtained by a procedure adapted from a reference²⁸ whereby a round-bottomed flask was charged with 2,2,2-trifluoroethanol (9.75 g, 111 mmol), NaOH (0.44 g, 11 mmol) and ethylene carbonate (9.75 g, 111 mmol). The mixture was refluxed at 110 °C overnight

and the product (14 g, 87 %) was collected by distillation. Next, PBr₃ was slowly added to the colourless liquid at 0 °C and stirred for 1 hour. The ice bath was then removed and the reaction mixture stirred for 3 hours. The resulting crude product was placed on ice and saturated NaHCO₃ was very carefully added. The lower layer was collected and distilled to yield the colourless product **S1.2** (8 g, 95 %). ¹H NMR (400 MHz, CDCl₃) δ 4.00-3.86 (m, 4H), 3.48 (td, J = 6.1, 2.0 Hz, 2H). ¹⁹F NMR (377 MHz, CDCl₃) δ -74.38 (t, J = 8.6 Hz). ¹³C NMR (101 MHz, CDCl₃) δ 123.91 (q, J = 279.6 Hz), 72.39 (s), 68.57 (q, J = 34.3 Hz), 29.42 (s). **S1.3** was synthesised as reported by Mansfeld and others.²⁹ In order to prepare **M1**, **S1.2** (2.8 g, 13.5 mmol) was stirred with K₂CO₃ (138.2, 7.4 mmol) and acetone (20 mL) for 30 min at 0 °C, before **S1.3** (2 g, 12.26 mmol) was added and the reaction mixture was stirred for 36 hours at 60 °C. Acetone was then removed by rotary evaporator, H₂O was added and the mixture extracted with DCM. The resulting oil was purified by column chromatography to provide the colourless product (2.8 g, 78 %). ¹H NMR (300 MHz, CDCl₃) δ 6.26 (t, J = 1.8 Hz, 2H), 3.86-3.73 (m, 4H), 3.73-3.63 (m, 2H), 3.30-3.19 (m, 2H), 2.67 (d, J = 1.2 Hz, 2H), 1.52-1.44 (m, 1H), 1.31 (d, J = 9.9 Hz, 1H). ¹⁹F NMR (282 MHz, CDCl₃) δ -74.22 (s). ¹³C NMR (75 MHz, CDCl₃) δ 177.89 (s), 137.78 (s), 123.76 (q, J = 279.5 Hz), 79.10-73.55 (m), 68.06 (s), 67.78 (q, J = 34.2 Hz), 47.79 (s), 45.24 (s), 42.55 (s), 37.40 (s). HRMS (ESI) *m/z* C₁₃H₁₅F₃NO₃ [M+H]⁺: calculated 290.1036, found 290.1003; C₁₃H₁₄F₃NO₃Na [M+Na]⁺: calculated 312.0824, found 312.0821.

Perfluoro-*tert*-butoxyethyl-*cis*-norbornene-*exo*-2,3-dicarboxiimide (M2). *N*-(Hydroxyethyl)-*cis*-norbornene-*exo*-2,3-dicarboxiimide (**S2**, 486 mg, 2.35 mmol) synthesized according to a previous procedure²⁶ and triphenylphosphine (738 mg, 2.81 mmol) were dissolved in dry THF (10 mL). Next, DIAD (446 μL, 2.81 mmol) predissolved in 8 mL THF was added dropwise to the reaction mixture over 5 min. Then, perfluoro-*tert*-butanol in 9 mL THF was added at 0 °C and stirred overnight at RT. The mixture was placed in the fridge for a few hours and the residual precipitate was removed. The crude material was purified by a column chromatography with hexane:ethyl acetate (4:1, v/v) and the product was obtained

as a white crystalline solid (800 mg, 83 %). ^1H NMR (300 MHz, CDCl_3) δ 6.22 (t, $J = 1.8$ Hz, 2H), 4.13 (t, $J = 5.3$ Hz, 2H), 3.74 (t, $J = 5.3$ Hz, 2H), 3.27-3.14 (m, 2H), 2.63 (d, $J = 1.3$ Hz, 2H), 1.49-1.38 (d, 1H), 1.19 (d, $J = 10.4$ Hz, 1H). ^{19}F NMR (282 MHz, CDCl_3) δ -70.66 (s). ^{13}C NMR (75 MHz, CDCl_3) δ 177.43 (s), 137.71 (s), 120.08 (q, $J = 293.3$ Hz), 79.60 (td, $J = 59.8, 29.9$ Hz), 78.12-75.17 (m), 65.71 (d, $J = 1.6$ Hz), 47.74 (s), 45.14 (s), 42.51 (s), 37.87 (s). HRMS (ESI) m/z $\text{C}_{15}\text{H}_{13}\text{F}_9\text{NO}_3$ $[\text{M}+\text{H}]^+$: calculated 426.0752, found 426.0743; $\text{C}_{15}\text{H}_{12}\text{F}_9\text{NO}_3\text{Na}$ $[\text{M}+\text{Na}]^+$: calculated 448.0572, found 448.0562.

General Synthesis Procedure for Bis(2-hydroxyethyl)aminopropylamino- (S3), OH-TEG-amino- (S4) and Methyl-TEG-amino-*cis*-norbornene-*exo*-2,3-dicarboxiimide (M7). *cis*-Norbornene-*exo*-2,3-dicarboxylic anhydride (1.1 equiv) and the amine (1.0 equiv) were charged into a reaction flask fitted with a reflux condenser. Next, anhydrous toluene and triethylamine (0.1 equiv) were added and stirred overnight at 110 °C. The reaction mixture was filtered and the crude product was purified by flash chromatography using ethyl acetate:methanol as eluent to obtain the title compounds as colourless oils (**S3**: 94 %, **S4**: 82 %, **M7**: 88 %). **S3**: ^1H NMR (300 MHz, CDCl_3) δ 6.25 (s, 2H), 3.62-3.45 (m, 6H), 3.23 (s, 4H), 2.66 (d, $J = 1.1$ Hz, 2H), 2.58 (s, 4H), 2.50 (s, 2H), 1.71 (q, $J = 6.9$ Hz, 2H), 1.52-1.45 (m, 1H), 1.16 (d, $J = 9.8$ Hz, 1H). ^{13}C NMR (75 MHz, CDCl_3) δ 178.38 (s), 137.78 (s), 59.65 (s), 56.26 (s), 52.00 (s), 47.81 (s), 45.11 (s), 42.74 (s), 36.51 (s), 25.44 (s). HRMS (ESI) m/z $\text{C}_{16}\text{H}_{25}\text{N}_2\text{O}_4$ $[\text{M}+\text{H}]^+$: calculated 309.1814, found 309.1810; $\text{C}_{16}\text{H}_{24}\text{N}_2\text{O}_4\text{Na}$ $[\text{M}+\text{Na}]^+$: calculated 331.1634, found 331.1626. **S4**: ^1H NMR (400 MHz, CDCl_3) δ 6.22 (s, 2H), 3.70-3.43 (m, 16H), 3.20 (s, 2H), 2.62 (s, 2H), 1.42 (d, $J = 9.8$ Hz, 1H), 1.29 (d, $J = 9.8$ Hz, 1H). ^{13}C NMR (75 MHz, CDCl_3) δ 178.04 (s), 137.82 (s), 72.54 (s), 70.83-70.25 (m), 69.87 (s), 66.93 (s), 61.69 (s), 47.81 (s), 45.25 (s), 42.71 (s), 37.76 (s). HRMS (ESI) m/z $\text{C}_{17}\text{H}_{25}\text{NO}_6\text{Na}$ $[\text{M}+\text{Na}]^+$: calculated 362.1580, found 362.1574. **M7**: ^1H NMR (400 MHz, CDCl_3) δ 6.27 (t, $J = 1.7$ Hz, 2H), 6.27 (t, $J = 1.7$ Hz, 2H), 3.72-3.48 (m, 16H), 3.36 (s, 3H), 3.28-3.17 (m, 2H), 2.66 (d, $J = 1.2$ Hz, 2H), 1.47 (d, $J = 9.9$ Hz, 1H), 1.35 (d, $J = 9.9$ Hz, 1H). ^{13}C NMR (75 MHz, CDCl_3) δ 178.11 (s), 137.94 (s), 77.48 (s),

77.33-77.03 (m), 76.84 (s), 72.05 (s), 70.81-70.53 (m), 70.00 (s), 67.01 (s), 59.13 (s), 47.94 (s), 45.39 (s), 42.83 (s), 37.87 (s). HRMS (ESI) m/z $C_{18}H_{28}NO_6$ $[M+H]^+$: calculated 354.1917, found 354.1914; $C_{18}H_{27}NO_6Na$ $[M+Na]^+$: calculated 376.1736, found 376.1729.

Bis(2-(2,2,2-trifluoroethoxy)ethyl)aminopropylamino-*cis*-norbornene-*exo*-2,3-dicarboxiimide (M3). Methanesulfonyl chloride was added dropwise to a solution of **S3** (2.0 g, 6.49 mmol) in dry DCM at 0 °C. After 15 min of stirring, the ice bath was removed and the mixture stirred for further 4 hours. Then, saturated sodium bicarbonate was added and the DCM phase was washed three times with water. The solvent was removed on rotavap and the mixture was dissolved in dry THF (10 mL) and placed on ice. A mixture of 2,2,2-trifluoroethanol and potassium *tert*-butoxide was then added dropwise, the reaction was brought to 70 °C and stirred overnight. Next, the solvent was removed, the crude product redissolved in ethyl acetate, washed three times with water and purified by flash chromatography with a hexane:ethyl acetate (1:1, v/v) mixture to yield a yellowish oil (1.4 g, 70 %). 1H NMR (300 MHz, $CDCl_3$) δ 6.28 (s, 2H), 3.84 (q, J = 8.8 Hz, 4H), 3.67 (t, J = 5.5 Hz, 4H), 3.50 (t, J = 7.4 Hz, 2H), 3.26 (s, 2H), 2.73 (t, J = 5.6 Hz, 4H), 2.66 (s, 2H), 2.56 (t, J = 6.8 Hz, 2H), 1.68 (p, J = 7.1 Hz, 2H), 1.50 (d, J = 9.8 Hz, 1H), 1.20 (d, J = 9.9 Hz, 1H). ^{19}F NMR (282 MHz, $CDCl_3$) δ -74.26 (s). ^{13}C NMR (75 MHz, $CDCl_3$) δ 178.00 (s), 137.79 (s), 124.02 (q, J = 279.6 Hz), 71.41 (s), 68.47 (q, J = 33.9 Hz), 54.07 (s), 52.94 (s), 47.77 (s), 45.14 (s), 42.67 (s), 36.75 (s), 25.76 (s). HRMS (ESI) m/z $C_{20}H_{27}F_6N_2O_4$ $[M+H]^+$: calculated 473.1875, found 473.1856; $C_{20}H_{26}F_6N_2O_4Na$ $[M+Na]^+$: calculated 495.1695, found 495.1674.

Bis(2-(perfluoro-*tert*-butoxy)ethyl)aminopropylamino-*cis*-norbornene-*exo*-2,3-dicarboxiimide (M4). A mixture of **S3** (2.0 g, 6.5 mmol), triphenylphosphine (4.9 g, 19 mmol) and perfluoro-*tert*-butyl alcohol (2.4 mL, 18 mmol) was dissolved in anhydrous diethyl ether under an atmosphere of argon. To this solution at 0 °C was added di-*tert*-butylazodicarboxylate (DBAD, 4.2 g, 18 mmol) in one portion. DBAD was used instead of DIAD as it was easier to remove from the crude product after the Mitsunobu reaction.

The reaction mixture was warmed to RT and stirred for 24 h. After the completion of the reaction as indicated by TLC, the suspension was placed in a fridge overnight and the resulting precipitate was filtered away. A solution of hydrogen chloride (6 mL) was added to the mixture and stirred for one hour. The precipitate was washed with 4 M HCl and diethyl ether. The product was purified by flash chromatography with hexane:ethyl acetate (4:1, v/v) to yield a colourless oil (800 mg, 81 %). ^1H NMR (400 MHz, CDCl_3) δ 6.30 (t, J = 1.8 Hz, 2H), 4.06 (t, J = 5.6 Hz, 4H), 3.55-3.45 (m, 2H), 3.32-3.26 (m, 2H), 2.87 (t, J = 5.7 Hz, 4H), 2.68 (d, J = 1.2 Hz, 2H), 2.60 (t, J = 7.0 Hz, 2H), 1.73-1.63 (m, 2H), 1.55-1.51 (m, 2H), 1.21 (d, J = 9.8 Hz, 2H). ^{19}F NMR (377 MHz, CDCl_3) δ -70.60 (s). ^{13}C NMR (75 MHz, CDCl_3) δ (101 MHz, CDCl_3) δ 177.94 (s), 137.81 (s), 120.33 (q, J = 293.6 Hz), 79.72 (dd, J = 59.3, 29.6 Hz), 68.71 (s), 53.68 (s), 52.88 (s), 47.79 (s), 45.17 (s), 42.62 (s), 36.36 (s), 26.01 (s). HRMS (ESI) m/z $\text{C}_{24}\text{H}_{23}\text{F}_{18}\text{N}_2\text{O}_4$ $[\text{M}+\text{H}]^+$: calculated 745.1370, found 745.1351; $\text{C}_{20}\text{H}_{26}\text{F}_6\text{N}_2\text{O}_4\text{Na}$ $[\text{M}+\text{Na}]^+$: calculated 767.1190, found 767.1174.

2,2,2-trifluoroethoxy-TEG-amino-*cis*-norbornene-*exo*-2,3-dicarboxiimide (M5).

Methanesulfonyl chloride was added dropwise to a solution of **S4** (212 mg, 0.6 mmol) in dry DCM at 0 °C. After 15 min of stirring, the ice bath was removed and the mixture stirred for further 1 hour. Then, the solvent was removed on rotavap and the product redispersed in ethyl acetate, filtrated and the filtrate collected. The product was redissolved in dry THF (10 mL) and placed on ice. A mixture of 2,2,2-trifluoroethanol and potassium *tert*-butoxide was then added dropwise. The reaction was brought to 70 °C and stirred overnight. Next, the solvent was removed, the crude material redissolved in ethyl acetate, washed three times with water and purified by flash chromatography with a hexane:ethyl acetate (1:1, v/v) mixture to yield a yellowish oil (160 mg, 61 %). ^1H NMR (400 MHz, CDCl_3) δ 6.28 (t, J = 1.7 Hz, 1H), 3.90 (q, J = 8.8 Hz, 1H), 3.78 (dd, J = 5.6, 3.6 Hz, 1H), 3.74-3.53 (m, 6H), 3.28-3.24 (m, 1H), 2.67 (d, J = 1.0 Hz, 1H), 1.47 (dd, J = 6.3, 4.9 Hz, 1H), 1.36 (d, J = 9.9 Hz, 1H). ^{19}F NMR (377 MHz, CDCl_3) δ -74.27 (s). ^{13}C NMR (75 MHz, CDCl_3) δ 178.00 (s), 137.84 (s), 127.07-121.53 (m), 71.95 (s), 70.64 (dd, J = 7.5, 6.0 Hz), 69.91 (s), 68.77 (d, J = 34.0 Hz),

66.92 (s), 47.83 (s), 45.29 (s), 42.72 (s), 37.76 (s). HRMS (ESI) m/z $C_{19}H_{27}F_3NO_6$ $[M+H]^+$: calculated 422.1790, found 422.1784; $C_{19}H_{26}F_3NO_6Na$ $[M+Na]^+$: calculated 444.1610, found 444.1600.

Perfluoro-*tert*-butoxy-TEG-amino-*cis*-norbornene-*exo*-2,3-dicarboxiimide (M6). **S4** (803 mg, 2.37 mmol) and triphenylphosphine (745 mg, 2.84 mmol) were dissolved in dry THF (10 mL). Next, DIAD (450 μ L, 2.84 mmol) predissolved in 8 mL THF was added dropwise over 5 min. Then, perfluoro-*tert*-butanol in 9 mL THF was added in one portion at 0 °C and stirred overnight at RT. The reaction mixture was placed in the fridge for a few hours and the residual precipitate was removed. The crude product was purified by flash chromatograph using hexane:ethyl acetate (4:1, v/v) and the product was obtained as a white solid (0.95 g, 72 %). 1H NMR (400 MHz, $CDCl_3$) δ 6.28 (d, $J = 1.7$ Hz, 1H), 4.15 (s, 1H), 3.77-3.53 (m, 8H), 3.26 (d, $J = 1.5$ Hz, 1H), 2.67 (s, 1H), 1.47 (d, $J = 1.3$ Hz, 1H), 1.36 (d, $J = 9.8$ Hz, 1H). ^{19}F NMR (377 MHz, $CDCl_3$) δ -70.37 (s). ^{13}C NMR (75 MHz, $CDCl_3$) δ 178.45 (s), 138.29 (s), 120.80 (m, $J = 293.3$ Hz), 71.52 (s), 71.10 (d, $J = 3.2$ Hz), 70.37 (s), 69.82 (d, $J = 15.0$ Hz), 67.37 (s), 48.29 (s), 45.74 (s), 43.16 (s), 38.21 (s). HRMS (ESI) m/z $C_{21}H_{24}F_9NO_6$ $[M+H]^+$: calculated 558.1538, found 558.1543; $C_{21}H_{24}F_9NO_6Na$ $[M+Na]^+$: calculated 580.1358, found 580.1351.

Ring-Opening Metathesis Polymerization (P#). Two Schlenk flasks loaded with either a monomer **M#** (100 mg) or **G3** catalyst (amount depended on the desired molecular weight of the resulting polymer) were evacuated and backfilled with argon three times. The deoxygenated **G3** was then dissolved in dry DCM (1 mL, degassed via three freeze-pump-thaw cycles) and added in one portion to the flask containing monomer dissolved in dry, degassed DCM (2 mL). After 30 minutes of stirring at RT, the active species were quenched with ethyl vinyl ether (0.5 mL) and the mixture was stirred for another 30 min. Polymers were precipitated into methanol or hexane multiple times. Residual ruthenium was removed by SiliaMetS DMT, which was in turn discarded by centrifugation and filtration. Nearly quantitative yields were obtained for the polymerization.

Ring-Opening Metathesis Polymerization of Statistical and Block Copolymers (P#-*stat*-P7, P#-*b*-P7). While the first Schlenk flask was loaded with **G3** catalyst (amount depended on the desired molecular weight), the second Schlenk flask contained either only monomer **M#** or a mixture of monomers **M#** and **M7**, depending on whether the desired copolymers were either block or statistical, respectively. A monomer ratio **M#**:**M7** of 1:1 was used for all copolymers, except for **P4-*stat*-P7** and **P4-*b*-P7**, in which case a ratio of 1:3 (**M4**:**M7**) was implemented. The Schlenk flasks were evacuated and backfilled with argon three times. The deoxygenated **G3** was then dissolved in dry DCM (1 mL, degassed via three freeze-pump-thaw cycles) and added in one portion to the flask containing monomer dissolved in dry, degassed DCM (2 mL). In the case of block copolymers, monomer **M7** was added after 30 minutes of stirring at RT. The mixture was stirred for another 30 minutes and the active species were quenched with ethyl vinyl ether (0.5 mL) as described above. The statistical copolymers, on the other hand, were stirred at RT for only 45 minutes before the catalyst was quenched with ethyl vinyl ether. Polymers were precipitated into methanol or hexane multiple times. Residual ruthenium was removed by SiliaMetS DMT, which was in turn discarded by centrifugation and filtration. Nearly quantitative yields were obtained for the polymerization.

Formation of Quaternary Ammonium Polymers (P3-QA, P4-QA). Polymers (**P3** or **P4**, 1 equiv by monomer) were dissolved in anhydrous acetone. After the addition of K_2CO_3 (1.5 equiv) and methyl iodide (20 equiv), the reaction mixture was stirred overnight at 50 °C. The polymers were filtered and dialysed against acetone.

Dihydroxylation of Polymeric Olefins (P#-OH, P#-*stat*-P7-OH, P#-*b*-P7-OH, P#-QA-OH). **Method A:** Polymers (1 equiv by monomer, 100 mg) were dispersed in acetone (4 mL) and stirred at RT. 4-methylmorpholine *N*-oxide (2.1 equiv) and $K_2OsO_4 \cdot 2H_2O$ (0.01 equiv) predissolved in H_2O (0.4 mL) were added consecutively and the mixture was stirred for 18 hours. Next, osmium was removed by stirring with SiliaMetS DMT for 2 hours. The mixture was then filtered directly into a dialysis bag and

dialysed against water for three days. The remaining silica was removed by centrifugation and filtration. **Method B:** $\text{CeCl}_3 \cdot 7\text{H}_2\text{O}$ (0.1 equiv) predissolved in H_2O (0.1 mL) was added to a suspension of NaIO_4 in H_2O (0.8 mL). The reaction mixture was stirred at RT and placed on ice as soon as the suspension turned yellow. $\text{RuCl}_3 \cdot \text{H}_2\text{O}$ (0.01 equiv) predissolved in H_2O (0.1 mL) and polymers (1 equiv by monomers) predissolved in acetonitrile (3 mL) and ethyl acetate (3 mL) were added consecutively. The reaction was vigorously stirred for further 60 min on ice, at which point a mixture of Na_2SO_3 and Na_2SO_4 was added. After stirring for 30 min, the precipitate was removed by centrifugation and filtration. The supernatant was dialysed against water for three days. **Method C:** The procedure for *syn* dihydroxylation was adapted from reference.³⁰ 5 mL of glacial acetic acid was added to a mixture of polymers (200 mg, 1 equiv by monomer), NaIO_4 (0.6 equiv) and LiBr (0.4 equiv). The reaction mixture was then heated to 95 °C and stirred for 12 h. Next, the polymers were extracted into the ethyl acetate phase and washed three times with aqueous NaHCO_3 . The solvent was evaporated on a rotavap, the polymers dissolved in methanol (10 mL), the pH of the reaction mixture neutralized and the polymers stirred with K_2CO_3 (10 equiv) at 50 °C. After 12 h of stirring, the resulting polymers were dialysed against methanol for one day and against ultrapure water for further 2 days.

^1H , ^{19}F and ^{13}C Nuclear Magnetic Resonance (NMR). ^1H , ^{19}F and ^{13}C NMR spectra were recorded at 25 °C on a Bruker Avance 300 (^1H NMR 300 MHz, ^{19}F NMR 282 MHz, ^{13}C NMR 75 MHz) or Bruker Avance 400 (^1H NMR 400 MHz, ^{19}F NMR 376 MHz, ^{13}C NMR 100 MHz) NMR spectrometer. Decoupled HMQC spectra were obtained at 25 °C on a Bruker Avance 400 NMR spectrometer in the phase-sensitive mode. 256 time increments were collected and linearly predicted to 1024, with 4 transients per increment and relaxation delay of 1.5 s. DOSY spectra were also obtained at 25 °C on a Bruker Avance 400 NMR spectrometer with a standard Bruker pulse program, `stegp1s`. Diffusion time, the number of gradient steps, relaxation and recovery delay were set to 1000 ms, 16, 3 s and 1 μs , respectively. Weight-average molecular weights were determined by DOSY as described by

Grubbs and colleagues,³¹ whereby PEG standards were used to obtain a calibration curve. TopSpin 3.2 software was used to process the HMQC and DOSY spectra.

¹⁹F NMR Relaxation Time Measurements. ¹⁹F NMR spectra of solutions were recorded without proton decoupling on a Bruker Avance 300 NMR spectrometer at fluorine frequency of 282 MHz. The samples were dissolved in D₂O with an average concentration of 2 mg/mL. The magnetic field was locked to D₂O, which was fully encapsulated within an internal capillary tube and all the spectra were acquired at 25 °C. ¹⁹F NMR longitudinal (T_1) and transverse (T_2) relaxation times were measured using the inversion recovery and Carr-Purcell-Meiboom-Gill (CPMG) techniques, respectively. Shimming was performed prior to each experiment in order to minimise the B_0 field inhomogeneity. ¹⁹F NMR spectra of solutions for relaxation time measurements were recorded using a 90° pulse of 9 μ s, an acquisition time of 0.98 s and a repetition delay of 5-10 s. The spectrum width was 50 kHz and 4k data points were collected. Typically, two acquisitions were accumulated to improve the signal-to-noise ratio. Bruker's TopSpin 3.2 software obtains a 1D spectrum for each τ value stored in a 2D data set, which was baseline corrected and phased for quantitative measurements. Integration, fitting and T_1 or T_2 calculations were performed with Bruker's Dynamics Center software. For ¹⁹F NMR signal-to-noise ratio measurements, the solution spectra at 282 or 376 MHz were measured under the following conditions: 16 scans, relaxation delay 1 s, 90° pulse width 9 μ s or 18 μ s and acquisition time 0.98 s or 0.73 s, respectively.

High-Resolution Accurate Mass Spectrometry. High-resolution and accurate mass spectra (HRMS) were acquired by electrospray ionization (ESI) on a Thermo Scientific LTQ Orbitrap XL equipped with a nano-electrospray ion source and a resolution of 10^5 at m/z 400.

Matrix Assisted Laser Desorption Ionization Time of Flight Mass Spectrometry (MALDI-ToF). MALDI-ToF was performed on a Bruker ultrafleXtreme instrument using 2-[(2E)-3-(4-tertbutylphenyl)-2-methylprop-2-enylidene] malononitrile (DCTB) as a matrix, polystyrene as a calibrant and silver trifluoroacetate as an ionizing salt. Spectra

were recorded with an accelerating voltage of 20 kV in the reflector positive ion mode. The solutions of matrix:sample:cationizing agent were combined in a 10:1:1 ratio (v/v/v). 1 μ L of the resulting solution was deposited onto the plate, dried and examined. Ions were detected in a m/z range of $2 \cdot 10^3$ - $2 \cdot 10^4$.

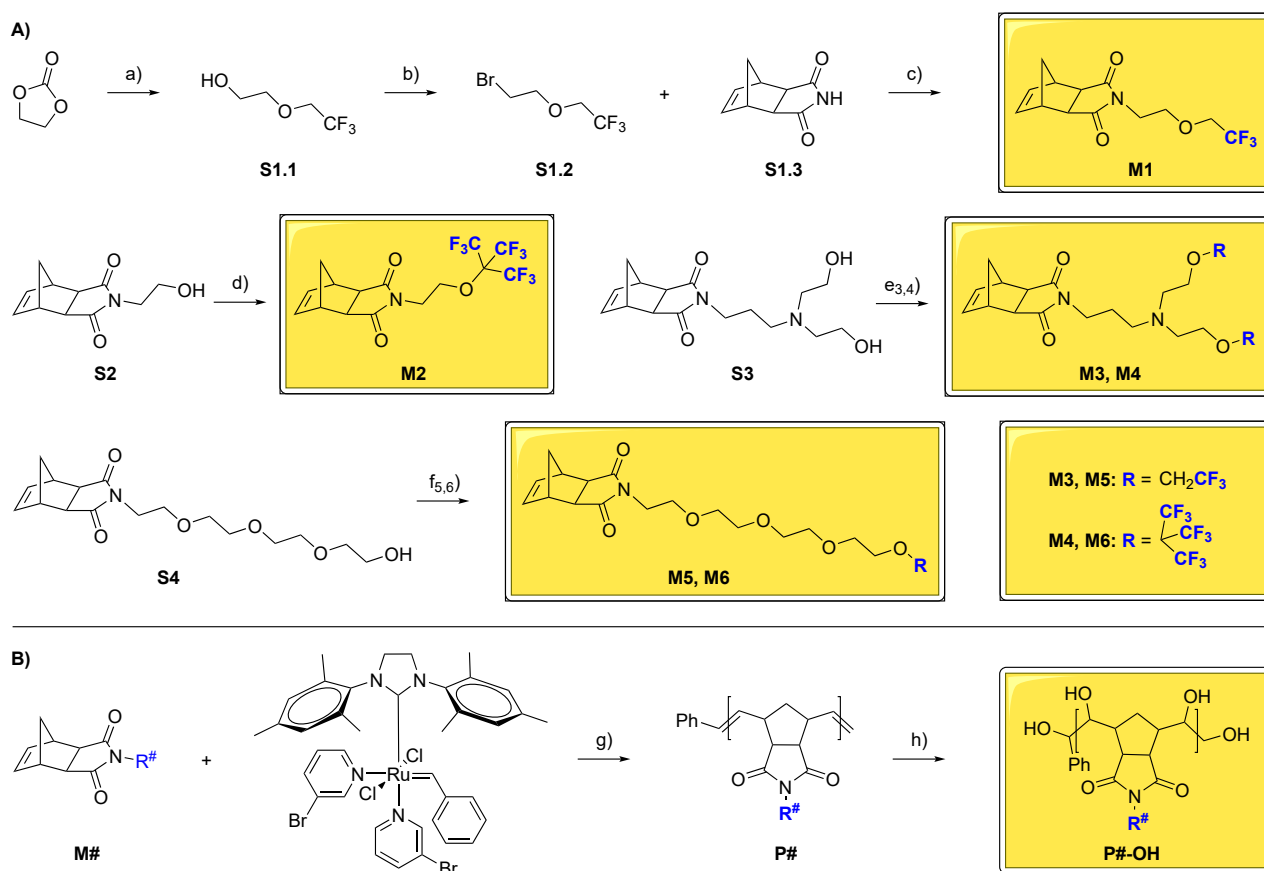
Gel permeation chromatography (GPC). The average relative molar mass (M_n , GPC) and molecular weight distribution ($\mathbb{D} = M_w/M_n$) values of polymers were determined by GPC in DMF (2 mg/mL) at RT and flow rate of 1 mL/min. The elution curves were calibrated with 10 monodisperse polystyrene standards (Malvern Polycal PS standards, MW range from 10^3 to $3 \cdot 10^6$ g/mol). For measurements in DMF, the GPC instrument was supplied with a Viscotek GPCmax VE2001 GPC solvent/sample module, a Viscotek UV detector 2600, a Viscotek VE3580 RI detector and two Viscotek T6000 M columns (7.8 \AA , 300 mm, 10^3 – 10^7 Da). All samples were dissolved in HPLC grade solvents, shaken overnight and filtered through a PTFE syringe membrane filter (0.45 μ m pore size, VWR) prior to GPC measurements. M_n values of polymers were not corrected for potential variations in the hydrodynamic diameters in DMF compared to the polystyrene standards.

Dynamic light scattering (DLS). DLS measurements were performed on a Beckman Coulter DelsaMax Series instrument. The scattering angle used was 90° and the temperature was fixed at 25 $^\circ$ C. Prior to measurements, the samples were dried and redispersed in ultrapure H_2O .

Results and Discussions

Fluorinated monomers based on *exo*-norbornene-imides that contain either 3 (**M1**, **M5**), 6 (**M3**), 9 (**M2**, **M6**) or 18 (**M4**) identical ^{19}F nuclei were designed in the form of one or more terminal trifluoromethyl groups (Scheme 1). In **M1** and **M2**, the fluorinated moieties were connected through a shorter alkyl linker to the imides, whereas in **M5** and **M6** a longer TEG-based linker was chosen. The pendants of terminal trifluoromethyl groups in **M3**

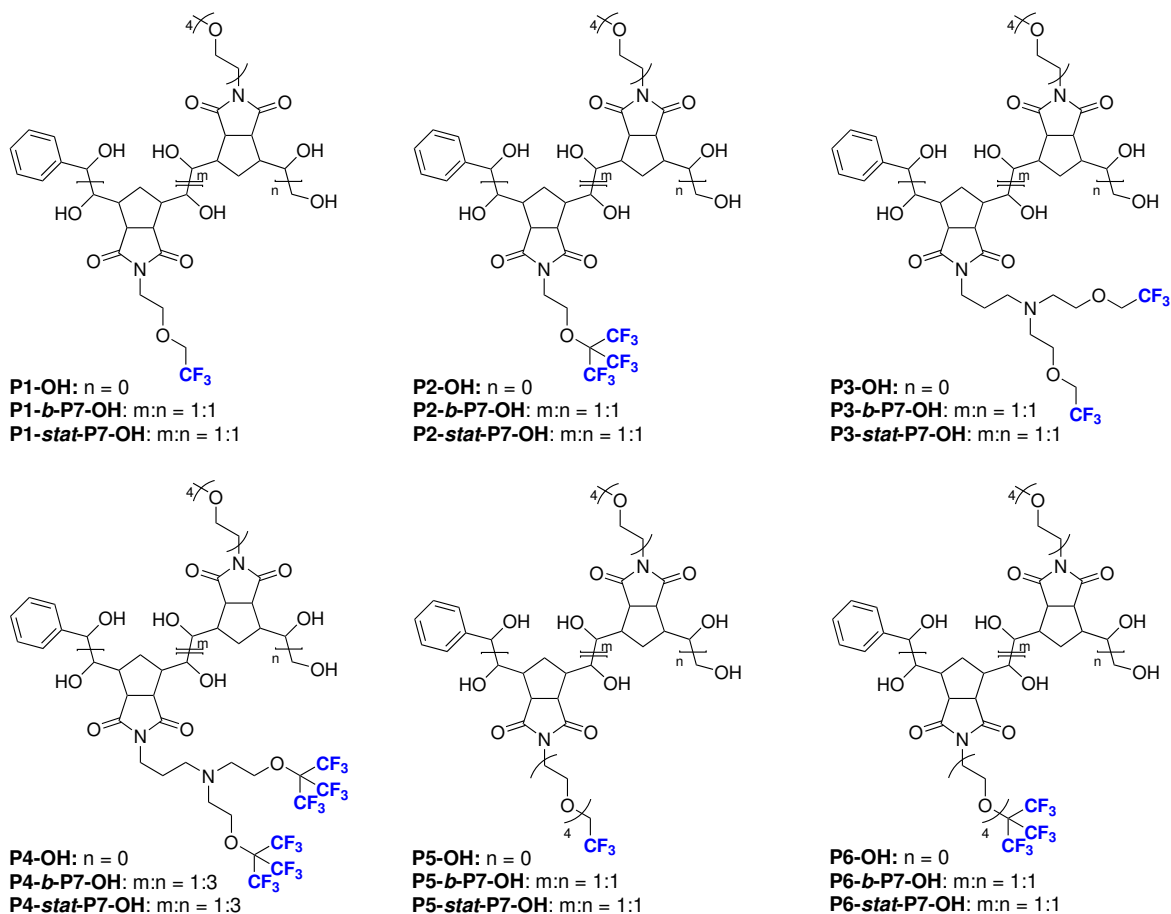
and **M4** are somewhat intermediary in length and incorporate a tertiary amine functionality. The corresponding homopolymers (**P1-P6**) were obtained by ROMP with Grubbs' 3rd generation catalyst (**G3**). Such ROMP polymers are intrinsically quite rigid due to their partially unsaturated backbone. Addition of a fluorinated moiety to the monomeric units further decreases their water solubility. In fact, even when olefin bonds are hydrogenated or when fluorinated monomers are copolymerized with TEG-substituted monomers they remain water-insoluble.



Scheme 1: Synthesis (A) and polymerization (B) of fluorinated monomers (**M1-M6**).^a
^aReagents and conditions: (a) CF₃CH₂OH, NaOH, 150 °C, 95 %; (b) PBr₃, 0 °C to RT; (c) K₂CO₃, acetone, RT to 60 °C, 78 % (over two steps); (d) (CF₃)₃COH, DIAD, PPh₃, THF, 0 °C to 40 °C, 83 %; (e₃) (i) CH₃SO₂Cl, N₃Et, DCM, 0 °C; (ii) CF₃CH₂OH, (CH₃)₃COK, THF, 0 °C to 70 °C, 70 %; (e₄) (CF₃)₃COH, DBAD, PPh₃, Et₂O, 0 °C to 40 °C, 81 %; (f₅) (i) CH₃SO₂Cl, N₃Et, DCM, 0 °C; (ii) CF₃CH₂OH, (CH₃)₃COK, THF, 0 °C to 70 °C, 61 %; (f₆) (CF₃)₃COH, DIAD, PPh₃, THF, 0 °C to 40 °C, 72 %; (g) (i) DCM, RT; (ii) C₂H₅OCH=CH₂; (h) NMO, K₂OsO₄·2H₂O, acetone, H₂O, RT.

Initially, LiBr-catalyzed NaIO₄-facilitated dihydroxylation of polymers (**P1-P4**) under acidic conditions³⁰ was attempted. All of the resulting polymers except **P2-OH-C** were

soluble in water and almost complete dihydroxylation could be shown by the missing olefin cross-peaks in the HMQC NMR spectra (Fig. S177-S178). Since molecular weight determination by GPC and DOSY was unfeasible due to insolubility in organic solvents and aggregation in water, respectively, the question of overoxidation-related C,C-bond cleavage remained unanswered.



Scheme 2: Chemical structures of fluorinated bishydroxylated homopolymers (**P#-OH**), block copolymers (**P#-*b*-P7-OH**) and statistical copolymers (**P#-*stat*-P7-OH**).

Thus, we embarked on an investigation of RuO_4 -catalyzed Lewis acid-facilitated dihydroxylation³² with metathesis-active ruthenium complexes such as **G3**. This would have been an excellent method to perform ROMP followed by dihydroxylation all in one-pot. Unfortunately, the dihydroxylation was only partial and accompanied by cleavage of the olefin bonds as shown by MALDI-ToF (Fig. S155-S166). The dihydroxylation efficiency improved

when **G3** was replaced with Grubbs' 2nd generation catalyst and became complete when RuCl_3 ³³ was implemented as a source of RuO_4 . Despite efforts to accelerate hydrolysis of ruthenate esters with CeCl_3 ,³⁴ C,C-bond cleavage could not be prevented.

The latter problem was avoided with classical Upjohn dihydroxylation, whereby *N*-methylmorpholine *N*-oxide was used to prepare OsO_4 *in situ*, while residual ruthenium and osmium were removed by silica-bound 2,4,6-trimercaptotriazine. The resulting polymers (**P1-OH** - **P6-OH**, Scheme 2) were slightly soluble in DMF and their molecular weights could be estimated by GPC (Fig. S179-S183). MALDI-ToF mass spectrum of **P2-OH** also indicated that after 18 hours the dihydroxylation was almost complete and that the C,C-bond cleavage did not occur (Fig. 1). Both **P2-OH** and **P4-OH** were insoluble in water due to perfluoro-*t*-butyl ethers and high fluorine content of 37 % and 43 %, respectively.

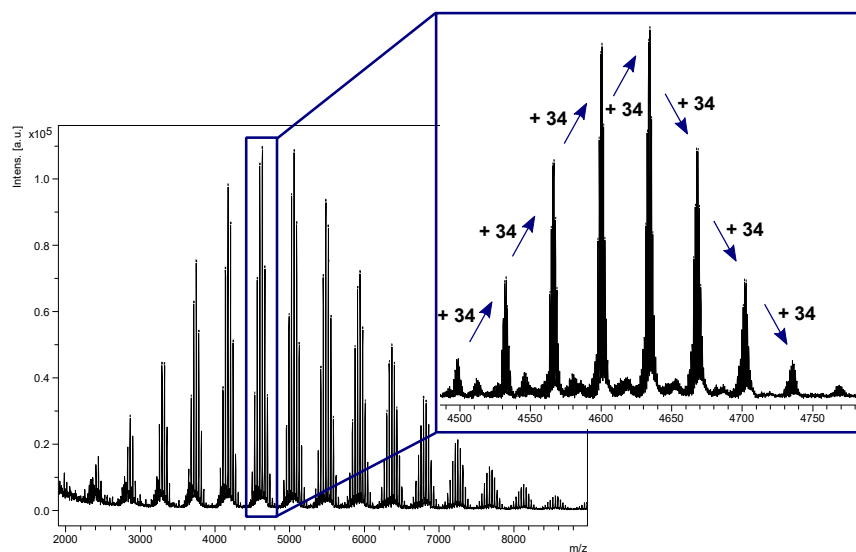


Figure 1: MALDI-ToF mass spectrum of **P2-OH**. The detected masses in the inset correspond to the increasing amount of dihydroxyl groups within a polymer chain. If C,C-bonds had been cleaved, the masses would have been 18 m/z apart as shown in supporting information (Fig. S165).

Similarly, very weak ¹⁹F NMR signals of **P1-OH**, **P3-OH** and **P6-OH** (with a fluorine content of 17 %, 22 % and 28 %, respectively) in water could only be obtained at low molecular weights (i.e., at 7 kDa, 12 kDa and 5 kDa, respectively). Further increase of the molecular weights completely attenuated the ¹⁹F NMR signal due to aggregation of fluori-

nated moieties. ^{19}F NMR signal-to-noise ratios (SNRs) of **P3-OH** improved substantially when tertiary amines were transformed into quaternary ammonium salts (**P3-QA-OH**, Table 1) by methylation with methyl iodide and slightly increased when the molecular weight of the parent olefin polymer was increased from 11 kDa to 32 kDa. In both cases, the ^{19}F NMR signal was linearly dependent on the polymer concentration (Fig. S233). Quaternization of **P4-OH**, on the other hand, did not contribute to its water solubility and ^{19}F NMR signal could not be detected in water.

Table 1: Physical and NMR properties of bishydroxylated polymers. For ^{19}F NMR relaxation time measurements (282 MHz, 298 K), the polymers were dissolved in water at a concentration of 2 mg/mL.

Polymer	$M_{w,NMR}^a$ [kDa]	$M_{n,GPC}^c$ [kDa]	\mathcal{D}^c	R_h^d [nm]	$^{19}\text{F } T_1$ [ms]	$^{19}\text{F } T_2$ [ms]	$^{19}\text{F } T_1/T_2$	Fluorine content [%]	^{19}F NMR SNR
P1-OH	7.1 ^b	6.9	1.18	81.8 ^e	1070 ± 237	239 ± 63	4.5	17	12
P3-OH	11.7 ^b	11.2	1.10	19.8 ^e	1245 ± 164	401 ± 127	3.1	22	15
P3-QA-OH	5.2	11.2	1.10	1.9	948 ± 42	381 ± 67	2.5	17	39
P5-OH	3.2	6.3	1.14	1.5	1716 ± 96	1071 ± 49	1.6	12	31
P6-OH	5.2 ^b	5.6	1.16	10.3 ^e	1626 ± 142	133 ± 45	12.2	28	11

^aMolecular weights of bishydroxylated polymers estimated by ^1H DOSY NMR in D_2O or by ^bGPC in DMF. $M_{w,NMR}$ was calculated from the PEG standard calibration curve using the experimental value of diffusion coefficient. ^cMolecular weights and poly dispersity indices (\mathcal{D}) of their parent non-dihydroxylated polymers. ^dHydrodynamic radii of bishydroxylated polymers calculated by the Stokes-Einstein equation from the diffusion coefficients of the polymers determined by ^1H DOSY NMR in D_2O or measured by ^eDLS in H_2O . ^1H DOSY and ^{19}F NMR SNRs were measured at 400 MHz and 376 MHz, respectively, at a polymer concentration of 0.5 mg/mL.

Compared to **P1-OH**, **P5-OH** yielded an excellent ^{19}F NMR signal in water and ^{19}F NMR T_1/T_2 ratio improved substantially from 4.5 to 1.6 (Table 1), which is excellent for homofluoropolymers. While the low ^{19}F NMR T_2 value of **P1-OH** was a consequence of shorter linkages between trifluoromethyl groups and the polymeric backbone, 4.5 times longer ^{19}F T_2 of **P5-OH** was a result of longer tetraethylene glycol linkers separating the fluorine moieties from the polymer main chain and thus faster internal motions. The glycol side chains also allowed for greater exposure to the solvent. Despite ^{19}F T_1/T_2 and SNR values increasing from 1.6 to 2.2 (Table S5) and decreasing by almost twofold (Table S6), respectively, when the molecular weight of their parent olefin polymers was increased from 13 to 56 kDa, the

^{19}F NMR SNRs of the highest molecular weight **P5-OH** were still linearly dependent on the polymer concentration (Fig. S235).

The question arose whether ^{19}F NMR relaxation times and SNRs of bishydroxylated polymers (**P#-OH**, Fig. 2) would improve at higher molecular weights with random incorporation of hydrophilic TEG-ylated monomers in 1:1 ratio. In the case of copolymers based on **M4** (18 equivalent fluorines per monomer), the ratio of TEG-ylated monomers had to be increased to three in order to not breach the 21 % fluorine content limit. All of the resulting statistical copolymers (**P#-stat-P7-OH**, Fig. 2) indeed exhibited higher ^{19}F SNRs and improved ^{19}F NMR T_1/T_2 ratios compared to their homofluoropolymeric counterparts (Table 1 and Table 2). In addition, all of the obtained ^{19}F SNRs were linearly dependent on polymer concentration in water. This was also true for copolymers with higher molecular weights (40-60 kDa). While the ^{19}F SNRs of **P2-stat-P7-OH**, **P3-stat-P7-OH** and **P4-stat-P7-OH** decreased with molecular weight, the ^{19}F SNRs of **P1-stat-P7-OH** and **P6-stat-P7-OH** remained constant and the ^{19}F SNR of **P5-stat-P7-OH** increased (cf. Fig. S230-S240, Table S6).

A comparison between trifluoromethyl- (i.e., **P1-stat-P7-OH**) and perfluoro-*t*-butyl- (i.e., **P2-stat-P7-OH**) functionalized copolymers again demonstrates that it is possible to achieve threefold lower ^{19}F NMR T_1/T_2 and 43 % higher signal-to-noise ratios despite 60 % lower fluorine content (Table 1 and Fig. 2). However, highly fluorinated units may still prove beneficial if larger amounts of non-fluorinated components are required especially at lower molecular weights. For example, similar ^{19}F NMR T_1/T_2 and signal-to-noise ratios were obtained (Table 1) when the TEG (**M7**) to bis-perfluoro-*t*-butylated monomer (**M4**, 18 equivalent fluorines) ratio was increased threefold in **P4-stat-P7-OH** compared to **P3-stat-P7-OH**, which contained TEG and bis-trifluoromethyl units (**M3**, 6 equivalent fluorines) in one-to-one ratio.

While the ^{19}F NMR signal was still detectable in statistical fluorinated copolymers (**P(1-4)-stat-P7-OH**) with molecular weights between 40 and 60 kDa, the ^{19}F resonance peak

Table 2: Physical and NMR properties of bishydroxylated statistical and block copolymers. For ^{19}F NMR relaxation time measurements (282 MHz, 298 K), the polymers were dissolved in water at a concentration of 2 mg/mL.

Polymer	$M_{w,NMR}^a$ [kDa]	$M_{n,GPC}^b$ [kDa]	\mathfrak{D}^b	R_h^c [nm]	$^{19}\text{F } T_1$ [ms]	$^{19}\text{F } T_2$ [ms]	$^{19}\text{F } T_1/T_2$	Fluorine content [%]	^{19}F NMR SNR
P1-<i>stat</i>-P7-OH	5.0	6.5	1.27	1.9	658 ± 21	263 ± 24	2.4	8	30
P1-<i>b</i>-P7-OH	4.7	6.2	1.21	3.1	696 ± 19	289 ± 17	2.5	8	30
P2-<i>stat</i>-P7-OH	9.6	5.4	1.21	3.2	478 ± 26	66 ± 15	7.2	20	21
P2-<i>b</i>-P7-OH	16.4	5.1	1.17	1.9	467 ± 20	64 ± 21	7.3	20	21
P3-<i>stat</i>-P7-OH	5.6	6.2	1.27	2.0	855 ± 73	352 ± 25	2.4	13	20
P3-<i>b</i>-P7-OH	4.3	5.5	1.44	1.7	361 ± 66	51 ± 19	7.1	13	14
P4-<i>stat</i>-P7-OH	12.6	5.3	1.19	4.5	471 ± 37	124 ± 29	3.8	17	28
P4-<i>b</i>-P7-OH	15.5	6.5	1.19	5.6	451 ± 50	82 ± 27	5.5	17	15
P5-<i>stat</i>-P7-OH	4.3	5.0	1.12	1.7	1685 ± 51	1215 ± 86	1.4	7	32
P5-<i>b</i>-P7-OH	5.3	5.0	1.14	2.0	1420 ± 66	979 ± 72	1.5	7	29
P6-<i>stat</i>-P7-OH	5.5	5.2	1.07	2.0	561 ± 45	54 ± 9	10.3	17	31
P6-<i>b</i>-P7-OH	20.0	5.6	1.16	10.6	547 ± 9	88 ± 8	6.2	17	34

^aMolecular weights of bishydroxylated polymers estimated by ^1H DOSY NMR in D_2O were calculated from the PEG standard calibration curve using the experimental value of diffusion coefficient. ^bMolecular weights and poly dispersity indices (\mathfrak{D}) of their parent non-dihydroxylated polymers. ^cHydrodynamic radii of bishydroxylated polymers calculated by the Stokes-Einstein equation from the diffusion coefficients of the polymers determined by ^1H DOSY NMR in D_2O . ^1H DOSY and ^{19}F NMR SNRs were measured at 400 MHz and 376 MHz, respectively, at a polymer concentration of 0.5 mg/mL.

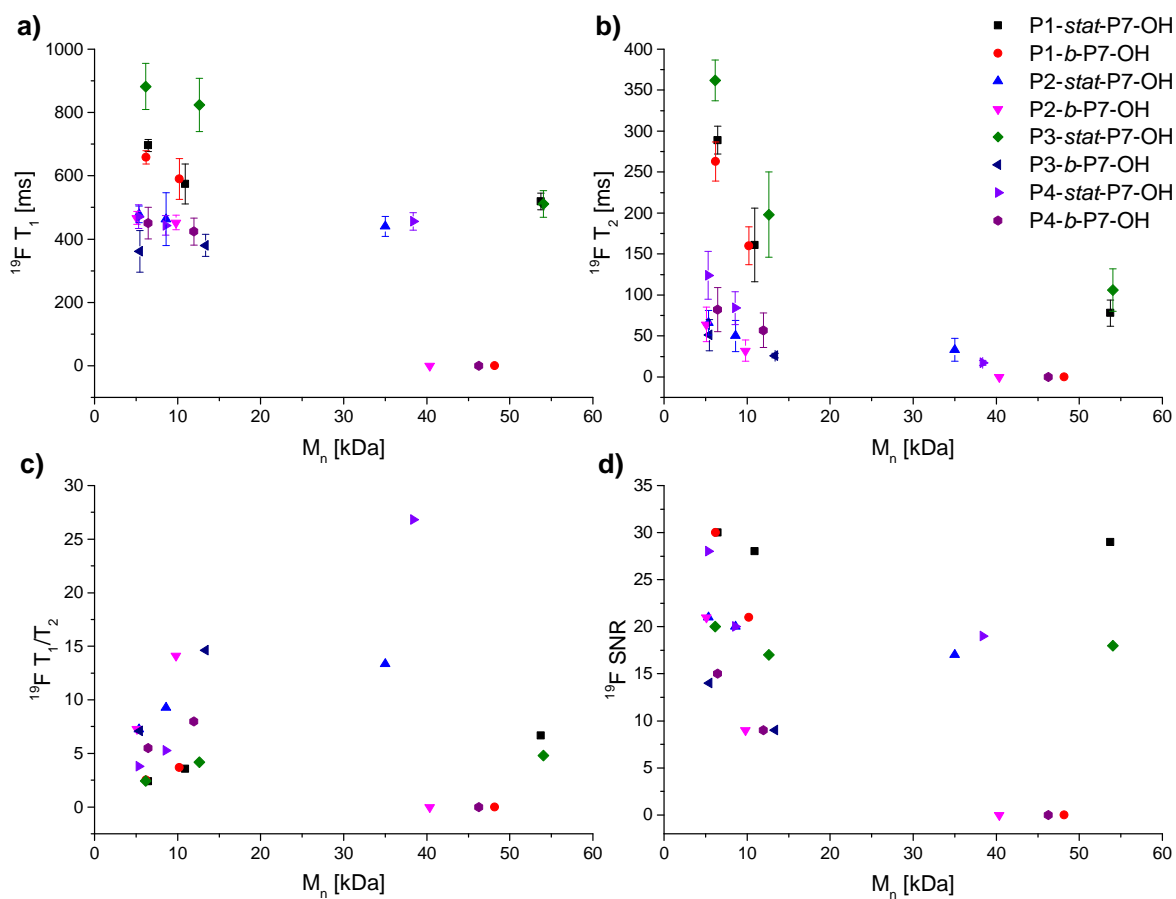


Figure 2: Comparison of a) ^{19}F NMR T_1 and b) T_2 relaxation times, c) ^{19}F NMR T_1/T_2 ratios and d) ^{19}F NMR SNR values of dihydroxylated statistical and block copolymers of various molecular weights in water. The ^{19}F NMR signal of **P(1-4)-*b*-P7-OH** block copolymers with a molecular weight larger than 35 kDa was not detected and thus the ^{19}F NMR relaxation properties were not measured.

completely disappeared in block copolymers (**P(1-4)-b-P7-OH**, Scheme 2) of comparable size (Fig. 2). At higher molecular weights, the fluorinated block probably self-assembles into a fluorous phase similarly to the homofluoropolymers, whereas the phase segregation of the fluorinated moieties in statistical copolymers is prevented by randomly distributed hydrophilic TEG chains. This was also shown in the case of a fluorinated TEG-based amphiphile by Yu and others.³⁵ At lower molecular weights, the differences in ^{19}F NMR relaxation properties between statistical and block copolymers were not found to be profound. This is true especially in **M1-**, **M2-** and **M5-** based statistical and block copolymers with a molecular weight of 5-6 kDa, where ^{19}F SNR and T_1/T_2 ratios were within error bars.

Since **P5-OH** was the only homofluoropolymer with ^{19}F NMR signal still detectable at high molecular weights, it is of no surprise that the corresponding block copolymers performed better at higher molecular weights than the **P(1-4)**-based block copolymers. The ^{19}F SNRs of **P5-b-P7-OH** remained constant when the molecular weight of the parent olefin polymers was increased from 5 kDa to 10 kDa. A decrease in ^{19}F NMR SNR similar to **P5-OH** was only observed when the molecular weight was increased to 50 kDa (Fig. 3). This is again most likely a consequence of strong dipolar couplings of the near-neighbouring ^{19}F nuclei.

The ^{19}F SNRs of **P5-*stat*-P7-OH**, on the other hand, increased slightly with molecular weight (cf. Fig. S236-S238) despite the subtle growth of ^{19}F NMR T_1/T_2 ratios from 1.4 to 1.7 (Table S5, Fig. 3). The rise of SNR was in a linear relationship with both the increasing fluorine content and the molecular weight (Fig. 4). Such linear dependence of ^{19}F NMR intensity on fluorine content in a wide range of molecular masses may be used for quantitative MRI. Whittaker and colleagues even observed rising ^{19}F NMR SNRs of discrete oligo(acrylic acid)s containing one terminal CF_3 group with longer chain length despite an increase in ^{19}F NMR T_1/T_2 ratios.³⁶ Out of all examined copolymers, **P5-*stat*-P7-OH** was also the one with the smallest growth in ^{19}F NMR T_1 (15 %) and T_2 (30 %) values when the molecular weight was increased from 5 kDa to 50 kDa.

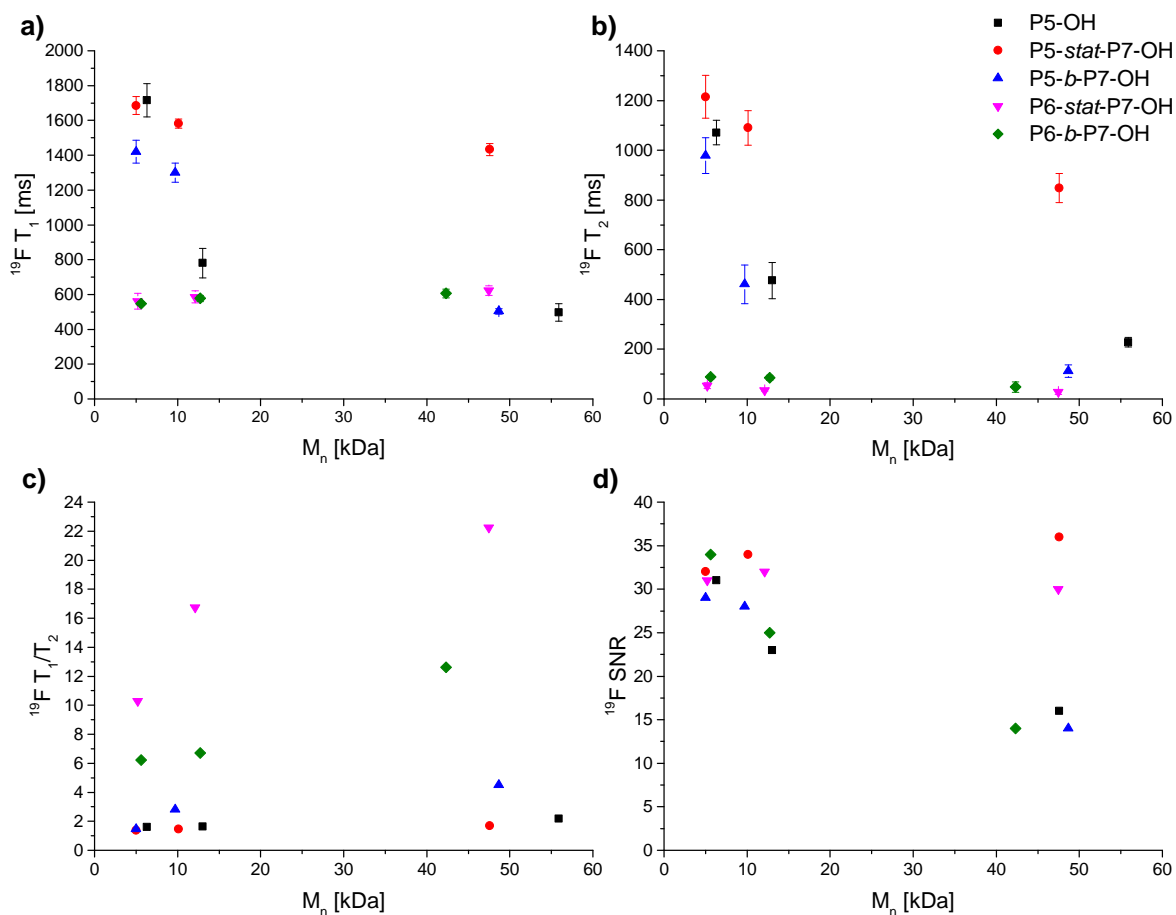


Figure 3: Comparison of water-soluble s and copolymers of different molecular weights. a) ^{19}F NMR T_1 and b) T_2 relaxation times, c) ^{19}F NMR T_1/T_2 ratios and d) ^{19}F NMR SNR values of dihydroxylated homofluoropolymer **P5-OH**, statistical and block copolymers of various molecular weights in water.

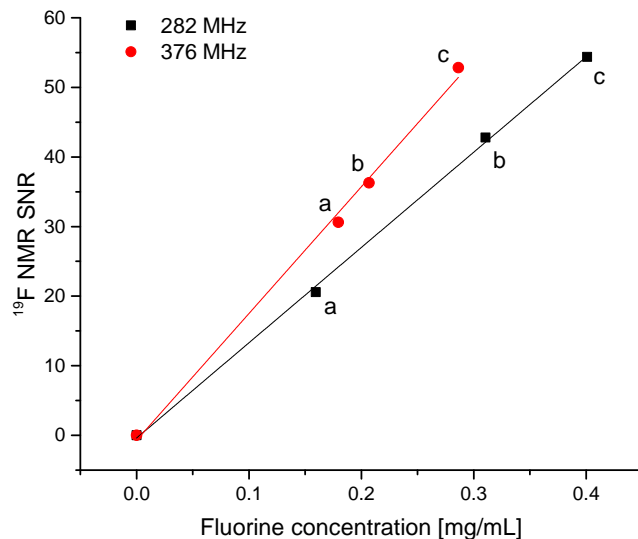


Figure 4: Linear relationship of ^{19}F NMR signal-to-noise ratios (282 and 376 MHz, 25 °C, $n_s = 16$, $l_b = 0.3$ Hz) of **P5-*stat*-P7-OH** copolymers with molecular weights of a) 5 kDa, b) 10 kDa and c) 50 kDa in D_2O .

The ^{19}F NMR T_1 and T_2 values of **P6-*stat*-P7-OH** and **P6-*b*-P7-OH** by contrast both increased by 11 % and about 47 %, respectively, with the tenfold rise of molecular weight (Table S4) due to very fast internal rotations of ^{19}F spins. In large macromolecules, these are known to result in longer longitudinal relaxation times with increasing molecular weight, whereas moderate rotations observed in **M1-5**-based copolymers improved the efficiency of spin-lattice relaxation and therefore shortened the T_1 values.³⁷ Although **P6-*b*-P7-OH** block copolymers showed lower ^{19}F NMR T_1/T_2 ratios than their statistical counterparts (Table S5, Fig. 3), **P6-*stat*-P7-OH** also exhibited better ^{19}F NMR SNRs with increasing molecular weights. Nevertheless, regarding the ^{19}F NMR relaxation properties especially at higher molecular weights, the examined fluorinated statistical copolymers performed better than the block copolymers, which were in turn superior to the homopolymers.

Conclusion

In summary, ring-opening metathesis polymerization quickly and efficiently provided narrowly-dispersed fluoropolymers bearing monomeric units of 3, 6, 9 or 18 magnetically equivalent

fluorine atoms. We found that dihydroxylation of the partially unsaturated polymeric backbone substantially improves their water solubility and ^{19}F NMR signal-to-noise ratio. This applies when the fluorine content does not exceed the 21 wt % limit and when the molecular weight is low. In the investigated homofluoropolymers, trifluoromethyl units thus exhibit better ^{19}F NMR signal-to-noise ratios than the perfluoro-*t*-butyl ones. The ^{19}F magnetic resonance properties further improve when longer water-solubilizing linkers between the fluorinated moieties and polymer main chain are incorporated as opposed to smaller, aliphatic connectors. A similar effect is achieved either by ammonium quaternization of linkers bearing tertiary amines or by copolymerization with tetraethylene glycol-substituted monomers, especially when the fluorine content is high. All these polymers exhibited ^{19}F NMR signal-to-noise ratios linearly dependent on polymer concentration. Furthermore, statistical copolymers composed of methyl- and trifluoromethyl-functionalized TEG-based monomers yielded a linear dependence of ^{19}F NMR intensity on fluorine content over a molecular weight range of 5 to 50 kDa and could thus find application as quantitative polymeric ^{19}F MRI contrast agents.

Acknowledgement

The authors thank NCCR Bio-inspired Materials for funding/financial support.

Supporting Information Available

Full experimental procedures.

This material is available free of charge via the Internet at <http://pubs.acs.org/>.

References

- (1) Luffer, R. B. Paramagnetic Metal Complexes as Water Proton Relaxation Agents for NMR Imaging: Theory and Design. *Chem. Rev.* **1987**, *87*, 901–927.
- (2) Fu, C.; Zhang, C.; Peng, H.; Han, F.; Baker, C.; Wu, Y.; Ta, H.; Whittaker, A. K. Enhanced Performance of Polymeric ¹⁹F MRI Contrast Agents through Incorporation of Highly Water-Soluble Monomer MSEA. *Macromolecules* **2018**, *51*, 5875–5882.
- (3) Knight, J. C.; Edwards, P. G.; Paisey, S. J. Fluorinated Contrast Agents for Magnetic Resonance Imaging; a Review of Recent Developments. *RSC Adv.* **2011**, *1*, 1415.
- (4) Wang, K.; Peng, H.; Thurecht, K. J.; Puttick, S.; Whittaker, A. K. pH-responsive star polymer nanoparticles: potential ¹⁹F MRI contrast agents for tumour-selective imaging. *Polymer Chemistry* **2013**, *4*, 4480–4489.
- (5) Jirak, D.; Galisova, A.; Kolouchova, K.; Babuka, D.; Hruby, M. Fluorine Polymer Probes for Magnetic Resonance Imaging: Quo Vadis? *Magn. Reson. Mat. Phys. Biol. Med.* **2019**, *32*, 173–185.
- (6) Diou, O.; Tsapis, N.; Giraudeau, C.; Valette, J.; Gueutin, C.; Bourasset, F.; Zanna, S.; Vauthier, C.; Fattal, E. Long-Circulating Perfluorooctyl Bromide Nanocapsules for Tumor Imaging by ¹⁹F MRI. *Biomaterials* **2012**, *33*, 5593–5602.
- (7) Janjic, J.; Srinivas, M.; Kadayakkara, D.; Ahrens, E. Self-Delivering Nanoemulsions for Dual Fluorine-¹⁹ MRI and Fluorescence Detection. *J. Am. Chem. Soc.* **2008**, *130*, 2832–2841.
- (8) Dardzinski, B.; Sotak, C. Rapid Tissue Oxygen Tension Mapping using ¹⁹F Inversion-Recovery Echo-Planar Imaging of Perfluoro-15-crown-5-ether. *Magn. Reson. Med.* **1994**, *32*, 88–97.

- (9) Tirotta, I.; Mastropietro, A.; Cordiglieri, C.; Gazzera, L.; Baggi, F.; Baselli, G.; Bruzzone, M.; Zucca, I.; Cavallo, G.; Terraneo, G.; Baldelli Bombelli, F. A Superfluorinated Molecular Probe for Highly Sensitive in Vivo ^{19}F -MRI. *J. Am. Chem. Soc.* **2014**, *136*, 8524–8527.
- (10) Neubauer, A. M.; Myerson, J.; Caruthers, S. D.; Hockett, F. D.; Winter, P. M.; Chen, J.; Gaffney, P. J.; Robertson, J. D.; Lanza, G. M.; Wickline, S. A. Gadolinium-Modulated ^{19}F Signals from Perfluorocarbon Nanoparticles as a New Strategy for Molecular Imaging. *Magn. Reson. Med.* **2008**, *60*, 1066–1072.
- (11) Jiang, Z.; Liu, X.; Jeong, E.; Yu, Y. Symmetry-Guided Design and Fluorous Synthesis of a Stable and Rapidly Excreted Imaging Tracer for ^{19}F MRI. *Angew. Chem. Int. Ed.* **2009**, *121*, 4849–4852.
- (12) Tanifum, E.; Patel, C.; Liaw, M.; Pautler, R.; Annapragada, A. Hydrophilic Fluorinated Molecules for Spectral ^{19}F MRI. *Sci. Rep.* **2018**, *8*, 2889.
- (13) Bo, S.; Song, C.; Li, Y.; Yu, W.; Chen, S.; Zhou, X.; Yang, Z.; Zheng, X.; Jiang, Z.-X. Design and Synthesis of Fluorinated Amphiphile as ^{19}F MRI/Fluorescence Dual-Imaging Agent by Tuning the Self-Assembly. *J. Org. Chem.* **2015**, *80*, 6360–6366.
- (14) Peng, H.; Blakey, I.; Dargaville, B.; Rasoul, F.; Rose, S.; Whittaker, A. K. Synthesis and Evaluation of Partly Fluorinated Block Copolymers as MRI Imaging Agents. *Biomacromolecules* **2009**, *10*, 374–381.
- (15) Huang, X.; Huang, G.; Zhang, S.; Sagiya, K.; Togao, O.; Ma, X.; Wang, Y.; Li, Y.; Soesbe, T.; Sumer, B.; Takahashi, M.; Sherry, D. A.; J., G. Multi-Chromatic pH-Activatable ^{19}F -MRI Nanoprobes with Binary ON/OFF pH Transitions and Chemical-Shift Barcodes. *Angew. Chem. Int. Ed.* **2013**, *52*, 8074–8078.
- (16) Rolfe, B.; Blakey, I.; Squires, O.; Peng, H.; Boase, N.; Alexander, C.; Parsons, P.; Boyle, G.; Whittaker, A.; Thurecht, K. Multimodal Polymer Nanoparticles with Com-

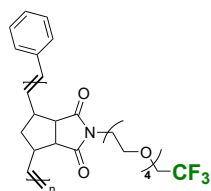
- bined ^{19}F Magnetic Resonance and Optical Detection for Tunable, Targeted, Multimodal Imaging in Vivo. *J. Am. Chem. Soc.* **2014**, *136*, 2413–2419.
- (17) Thurecht, K.; Blakey, I.; Peng, H.; Squires, O.; Hsu, S.; Alexander, C.; Whittaker, A. Functional Hyperbranched Polymers: Toward Targeted in Vivo ^{19}F Magnetic Resonance Imaging Using Designed Macromolecules. *J. Am. Chem. Soc.* **2010**, *132*, 5335–5337.
- (18) Fu, C. et al. Low-Fouling Fluoropolymers for Bioconjugation and In Vivo Tracking. *Angewandte Chemie* **2020**, *132*, 4759–4765.
- (19) Hilf, S.; Kilbinger, A. Functional End Groups for Polymers Prepared Using Ring-Opening Metathesis Polymerization. *Nat. Chem.* **2009**, *1*, 537.
- (20) Matson, J.; Grubbs, R. Synthesis of Fluorine-18 Functionalized Nanoparticles for Use as in Vivo Molecular Imaging Agents. *J. Am. Chem. Soc.* **2008**, *130*, 6731–6733.
- (21) Randolph, L.; LeGuyader, C.; Hahn, M.; Andolina, C.; Patterson, J.; Mattrey, R.; Millstone, J.; Botta, M.; Scadeng, M.; Gianneschi, N. Polymeric Gd-DOTA Amphiphiles form Spherical and Fibril-Shaped Nanoparticle MRI Contrast Agents. *Chem. Sci.* **2016**, *7*, 4230–4236.
- (22) Sowers, M.; McCombs, J.; Wang, Y.; Paletta, J.; Morton, S.; Dreaden, E.; Boska, M.; Ottaviani, M.; Hammond, P.; Rajca, A.; Johnson, J. Redox-Responsive Branched-Bottlebrush Polymers for in Vivo MRI and Fluorescence Imaging. *Nat. Commun.* **2014**, *5*, 5460.
- (23) Meier, S.; Reisinger, H.; Haag, R.; Mecking, S.; Mülhaupt, R.; Stelzer, F. Carbohydrate Analogue Polymers by Ring Opening Metathesis Polymerisation (ROMP) and Subsequent Catalytic Dihydroxylation. *Chem. Commun.* **2001**, *9*, 855–856.

- (24) Carrillo, A.; Gujraty, K. V.; Rai, P. R.; Kane, R. S. Design of Water-Soluble, Thiol-Reactive Polymers of Controlled Molecular Weight: a Novel Multivalent Scaffold. *Nanotechnology* **2005**, *16*, S416–S421.
- (25) Miki, K.; Kimura, A.; Oride, K.; Kuramochi, Y.; Matsuoka, H.; Harada, H.; Hiraoka, M.; Ohe, K. High-Contrast Fluorescence Imaging of Tumors In Vivo Using Nanoparticles of Amphiphilic Brush-Like Copolymers Produced by ROMP. *Angew. Chem. Int. Ed.* **2011**, *50*, 6567–6570.
- (26) Qiao, Y.; Ping, J.; Tian, H.; Zhang, Q.; Zhou, S.; Shen, Z.; Zheng, S.; Fan, X. Synthesis and Phase Behavior of a Polynorbornene-Based Molecular Brush with Dual "Jacketing" Effects. *J. Polym. Sci. Pol. Chem.* **2015**, *53*, 2116–2123.
- (27) Walton, H. M. Potential Antimicrobial Agents. III. 4-Methylamino-2, 4-alkadienoic Acid γ -Lactams¹. *J. Org. Chem.* **1956**, *22*, 315–318.
- (28) Mei, X.; Yue, Z.; Tufts, J.; Dunya, H.; Mandal, B. Synthesis of New Fluorine-Containing Room Temperature Ionic Liquids and their Physical and Electrochemical Properties. *J. Fluor. Chem.* **2018**, *212*, 26–37.
- (29) Mansfeld, F.; Feng, G.; Otto, S. Photo-Induced Molecular-Recognition-Mediated Adhesion of Giant Vesicles. *Org. Biomol. Chem.* **2009**, *7*, 4289–4295.
- (30) Emmanuvel, L.; Shaikh, T.; Sudalai, A. NaIO₄/LiBr-Mediated Diastereoselective Dihydroxylation of Olefins: A Catalytic Approach to the Prevost-Woodward reaction. *Org. Lett.* **2005**, *7*, 5071–5074.
- (31) Li, W.; Chung, H.; Daeffler, C.; Johnson, J. A.; Grubbs, R. H. Application of 1H DOSY for facile measurement of polymer molecular weights. *Macromolecules* **2012**, *45*, 9595–9603.

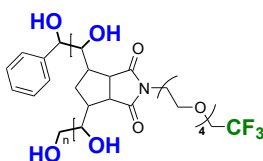
- (32) Scholte, A.; An, M.; Snapper, M. Ruthenium-Catalyzed Tandem Olefin Metathesis-Oxidations. *Org. Lett.* **2006**, *8*, 4759–4762.
- (33) Plietker, B.; Niggemann, M. An Improved Protocol for the RuO₄-Catalyzed Dihydroxylation of Olefins. *Org. Lett.* **2003**, *5*, 3353–3356.
- (34) Plietker, B.; Niggemann, M. RuCl₃/CeCl₃/NaIO₄: A New Bimetallic Oxidation System for the Mild and Efficient Dihydroxylation of Unreactive Olefins. *J. Org. Chem.* **2005**, *70*, 2402–2405.
- (35) Taraban, M.; Yu, L.; Feng, Y.; Jouravleva, E.; Anisimov, M.; Jiang, Z.; Yu, Y. Conformational Transition of a Non-Associative Fluorinated Amphiphile in Aqueous Solution. *RSC Adv.* **2014**, *4*, 54565–54575.
- (36) Zhang, C.; Kim, D. S.; Lawrence, J.; Hawker, C. J.; Whittaker, A. K. Elucidating the Impact of Molecular Structure on the ¹⁹F NMR Dynamics and MRI Performance of Fluorinated Oligomers. *ACS Macro Lett.* **2018**, *7*, 921–926.
- (37) Hull, W. E.; Sykes, B. D. Fluorotyrosine Alkaline Phosphatase: Internal Mobility of Individual Tyrosines and the Role of Chemical Shift Anisotropy as a ¹⁹F Nuclear Spin Relaxation Mechanism in Proteins. *J. Mol. Biol.* **1975**, *98*, 121–153.

Graphical TOC Entry

Ring-opening metathesis polymerization followed by dihydroxylation of olefins was employed to prepare hydrophilic fluorinated polymers with high stability in water. Excellent ^{19}F magnetic resonance properties could be obtained with the bishydroxylated non-ionic homo- and copolymers containing longer water-soluble linkages connecting trifluoromethyl groups in the monomeric units with the polymeric backbone. This technique is likely to spur a new range of quantitative, tracking, targeting and stimuli-responsive MRI contrast agents.



✗ Water-Insoluble
✗ No ^{19}F NMR Signal



↑ Water-Soluble
↑ ^{19}F NMR Signal